Journal of Zhejiang University-SCIENCE C (Computers & Electronics)
ISSN 1869-1951 (Print); ISSN 1869-196X (Online)
www.zju.edu.cn/jzus; www.springerlink.com
E-mail: jzus@zju.edu.cn

An efficient measurement-driven sequential Monte Carlo multi-Bernoulli filter for multi-target filtering*

Tong-yang JIANG[1,2], Mei-qin LIU‡[1,2], Xie WANG[2], Sen-lin ZHANG[2]

([1]*State Key Laboratory of Industrial Control Technology, Zhejiang University, Hangzhou 310027, China*)

([2]*College of Electrical Engineering, Zhejiang University, Hangzhou 310027, China*)

E-mail: {jiangtongyang, liumeiqin, wangxiek, slzhang}@zju.edu.cn

Received Jan. 25, 2014; Revision accepted Apr. 3, 2014; Crosschecked May 4, 2014

Abstract: We propose an efficient measurement-driven sequential Monte Carlo multi-Bernoulli (SMC-MB) filter for multi-target filtering in the presence of clutter and missing detection. The survival and birth measurements are distinguished from the original measurements using the gating technique. Then the survival measurements are used to update both survival and birth targets, and the birth measurements are used to update only the birth targets. Since most clutter measurements do not participate in the update step, the computing time is reduced significantly. Simulation results demonstrate that the proposed approach improves the real-time performance without degradation of filtering performance.

Key words: Measurement-driven, Gating technique, Sequential Monte Carlo, Multi-Bernoulli filter, Multi-target filtering

doi:10.1631/jzus.C1400025 **Document code:** A **CLC number:** TP391

1 Introduction

Recently, random finite set (RFS) based approaches have attracted more attention in multi-target tracking. Mahler's finite set statistics (FISST) (Mahler, 2007b) provides a rigorous Bayesian framework for multi-target filtering. The probability hypothesis density (PHD) (Mahler, 2003) and cardinalized PHD (CPHD) (Mahler, 2007a) filters have been derived for multi-target filtering. They can estimate both the target states and the number of targets without complex data association. The sequential Monte Carlo (SMC) and Gaussian mixture (GM) techniques have been implemented for the PHD and CPHD filters (Vo BN *et al.*, 2005; Vo and Ma, 2006; Vo BT *et al.*, 2007). In addition to the PHD and CPHD filters, Mahler (2007b) proposed the multi-target multi-Bernoulli (MeMBer) recursion as a tractable approximation to the Bayesian multi-target recursion using a multi-Bernoulli RFS. Unlike PHD and CPHD recursions, MeMBer recursion propagates the approximate posterior multi-target density. The advantage of multi-Bernoulli representation is that each Bernoulli distribution represents a hypothesized track and its existence probability, so the MeMBer filter allows reliable and inexpensive extraction of the state estimates. However, it is shown that the MeMBer filter overestimates the number of targets. To solve this problem, Vo (2008) and Vo *et al.* (2009) proposed the cardinality balanced MeMBer (CBMeMBer) filter by modifying the measurement updated track parameters, which has

‡ Corresponding author

* Project supported by the National Natural Science Foundation of China (Nos. 61174142, 61222310, and 61374021), the Specialized Research Fund for the Doctoral Program of Higher Education of China (Nos. 20120101110115 and 20130101110109), the Zhejiang Provincial Science and Technology Planning Projects of China (No. 2012C21044), the Marine Interdisciplinary Research Guiding Funds for Zhejiang University (No. 2012HY009B), the Fundamental Research Funds for the Central Universities (No. 2014XZZX003-12), and the Aeronautical Science Foundation of China (No. 20132076002)

an unbiased estimate of the number of targets.

The multi-Bernoulli filter has been applied for tracking with audio and video information (Hoseinnezhad *et al.*, 2011), tracking in sensor networks (Wei and Zhang, 2009; 2010a; 2010b; Gostar *et al.*, 2013a; 2013b; Hoang and Vo, 2014) and tracking from image information (Vo *et al.*, 2010; Hoseinnezhad *et al.*, 2013). Various implementations and extensions have been considered in Yin *et al.* (2010), Yin and Zhang (2010), Vo *et al.* (2011; 2013), Ravindra *et al.* (2012), and Baser *et al.* (2013). Hybrid multi-Bernoulli and Poisson multi-target filters were proposed in Williams (2012). The latest development is the exact closed-form solution or conjugate result known as the generalized labeled multi-Bernoulli (GLMB) filter, which also produces target tracks (Vo and Vo, 2013). The CBMeMber filter will be treated as a multi-Bernoulli (MB) filter throughout this paper.

Both GM and SMC techniques have been implemented for the MB filter (Vo, 2008; Vo *et al.*, 2009). Although the GM-MB filter has a closed-form solution, its application is constrained to linear Gaussian models. In contrast, the SMC-MB filer can be applied to nonlinear non-Gaussian models. The SMC-MB filter also outperforms SMC-PHD and SMC-CPHD filters (Vo *et al.*, 2009). The convergence results for the SMC-MB filter have been established in Lian *et al.* (2012). However, the computing time of the SMC-MB filter grows linearly with the increase of the amount of measurements. Specifically, in clutter environments, a lot of clutter measurements are included. If all the measurements are considered in the update step, more time will be consumed. Clutter measurements may also degrade the filtering accuracy. To avoid clutter measurements and reduce the computing time, an efficient measurement-driven SMC-MB filter is proposed in this paper. The novelty lies in that we distinguish the survival and birth measurements from the original measurements to update the target state. The main contributions of this paper can be summarized as follows:

1. We present an analysis of the time consumption of the prediction, update, and resampling steps, respectively, for SMC-MB recursion from the results of Monte Carlo (MC) simulation.

2. We use the gating technique for both survival and birth targets to distinguish survival and birth measurements.

3. We propose an efficient measurement-driven approach for the SMC-MB filter. The survival measurements are used to update both survival and birth targets, and the birth measurements are used to update only birth targets.

2 Analysis of time consumption for the SMC-MB filter

2.1 SMC-MB recursion

The SMC-MB filter has been proposed in Vo (2008) and Vo *et al.* (2009). Here, we summarize one cycle of the SMC-MB filtering algorithm.

Let $\{(r_{k-1}^{(i)}, p_{k-1}^{(i)})\}_{i=1}^{M_{k-1}}$ denote the posterior multi-target density at time $k-1$, where $p_{k-1}^{(i)}$, the probability density of the ith hypothesized track, is composed of a set of weighted samples $\{w_{k-1}^{(i,j)}, \boldsymbol{x}_{k-1}^{(i,j)}\}_{j=1}^{L_{k-1}^{(i)}}$, i.e.,

$$p_{k-1}^{(i)}(\boldsymbol{x}) = \sum_{j=1}^{L_{k-1}^{(i)}} w_{k-1}^{(i,j)} \delta(\boldsymbol{x} - \boldsymbol{x}_{k-1}^{(i,j)}), \tag{1}$$

$r_{k-1}^{(i)}$ denotes the existence probability of the ith hypothesized track, M_{k-1} denotes the number of hypothesized tracks, $L_{k-1}^{(i)}$ denotes the number of particles for the ith hypothesized track at time $k-1$, and $\delta(\boldsymbol{x} - \boldsymbol{x}_{k-1}^{(i,j)})$ denotes the Dirac delta function centered at $\boldsymbol{x}_{k-1}^{(i,j)}$.

Let $\{(r_{\Gamma,k}^{(i)}, p_{\Gamma,k}^{(i)})\}_{i=1}^{M_{\Gamma,k}}$ denote the parameters of MB-RFS for birth targets at time k, where $p_{\Gamma,k}^{(i)}$, the probability density of the ith birth track, is composed of a set of weighted samples $\{w_{\Gamma,k}^{(i,j)}, \boldsymbol{x}_{\Gamma,k}^{(i,j)}\}_{j=1}^{L_{\Gamma,k}^{(i)}}$, i.e.,

$$p_{\Gamma,k}^{(i)}(\boldsymbol{x}) = \sum_{j=1}^{L_{\Gamma,k}^{(i)}} w_{\Gamma,k}^{(i,j)} \delta(\boldsymbol{x} - \boldsymbol{x}_{\Gamma,k}^{(i,j)}), \tag{2}$$

$r_{\Gamma,k}^{(i)}$ denotes the existence probability of the ith birth track, $M_{\Gamma,k}$ denotes the number of birth tracks at time k, and $L_{\Gamma,k}^{(i)}$ denotes the number of particles for the ith birth track at time k.

One cycle of SMC-MB recursion consists of three steps: prediction, update, and resampling.

1. Prediction

Given the posterior multi-target density

$$\pi_{k-1} = \{(r_{k-1}^{(i)}, p_{k-1}^{(i)})\}_{i=1}^{M_{k-1}} \tag{3}$$

at time $k-1$, the predicted multi-target density

$$\pi_{k|k-1}=\{r^{(i)}_{\mathrm{P},k|k-1},p^{(i)}_{\mathrm{P},k|k-1}\}_{i=1}^{M_{k-1}}\cup\{r^{(i)}_{\Gamma,k},p^{(i)}_{\Gamma,k}\}_{i=1}^{M_{\Gamma,k}} \tag{4}$$

can be computed as follows:

$$r^{(i)}_{\mathrm{P},k|k-1}=r^{(i)}_{k-1}\sum_{j=1}^{L^{(i)}_{k-1}}w^{(i,j)}_{k-1}p_{\mathrm{S},k}(\boldsymbol{x}^{(i,j)}_{k-1}), \tag{5}$$

$$p^{(i)}_{\mathrm{P},k|k-1}(\boldsymbol{x})=\sum_{j=1}^{L^{(i)}_{k-1}}w^{(i,j)}_{\mathrm{P},k|k-1}\delta(\boldsymbol{x}-\boldsymbol{x}^{(i,j)}_{\mathrm{P},k|k-1}), \tag{6}$$

$$p^{(i)}_{\Gamma,k}(\boldsymbol{x})=\sum_{j=1}^{L^{(i)}_{\Gamma,k}}w^{(i,j)}_{\Gamma,k}\delta(\boldsymbol{x}-\boldsymbol{x}^{(i,j)}_{\Gamma,k}), \tag{7}$$

where

$$\boldsymbol{x}^{(i,j)}_{\mathrm{P},k|k-1}\sim q^{(i)}_k(\cdot|\boldsymbol{x}^{(i,j)}_{k-1},Z_k),j=1,2,\cdots,L^{(i)}_{k-1}, \tag{8}$$

$q^{(i)}_k(\cdot|\boldsymbol{x}^{(i,j)}_{k-1},Z_k)$ are the importance (or proposal) densities for survival targets,

$$\tilde{w}^{(i,j)}_{\mathrm{P},k|k-1}=\frac{w^{(i,j)}_{k-1}f_{k|k-1}(\boldsymbol{x}^{(i,j)}_{\mathrm{P},k|k-1}|\boldsymbol{x}^{(i,j)}_{k-1})p_{\mathrm{S},k}(\boldsymbol{x}^{(i,j)}_{k-1})}{q^{(i)}_k(\boldsymbol{x}^{(i,j)}_{\mathrm{P},k|k-1}|\boldsymbol{x}^{(i,j)}_{k-1},Z_k)}, \tag{9}$$

$$w^{(i,j)}_{\mathrm{P},k|k-1}=\frac{\tilde{w}^{(i,j)}_{\mathrm{P},k|k-1}}{\sum_{j=1}^{L^{(i)}_{k-1}}\tilde{w}^{(i,j)}_{\mathrm{P},k|k-1}}, \tag{10}$$

$$\boldsymbol{x}^{(i,j)}_{\Gamma,k}\sim b^{(i)}_k(\cdot|Z_k),j=1,2,\cdots,L^{(i)}_{\Gamma,k}, \tag{11}$$

$b^{(i)}_k(\cdot|Z_k)$ are the importance (or proposal) densities for birth targets, and

$$\tilde{w}^{(i,j)}_{\Gamma,k}=\frac{p_{\Gamma,k}(\boldsymbol{x}^{(i,j)}_{\Gamma,k})}{b^{(i)}_k(\boldsymbol{x}^{(i,j)}_{\Gamma,k}|Z_k)}, \tag{12}$$

$$w^{(i,j)}_{\Gamma,k}=\frac{\tilde{w}^{(i,j)}_{\Gamma,k}}{\sum_{j=1}^{L^{(i)}_{\Gamma,k}}\tilde{w}^{(i,j)}_{\Gamma,k}}. \tag{13}$$

2. Update

Given the predicted multi-target density

$$\pi_{k|k-1}=\{(r^{(i)}_{k|k-1},p^{(i)}_{k|k-1})\}_{i=1}^{M_{k|k-1}} \tag{14}$$

at time k where each $p^{(i)}_{k|k-1}$ is composed of a set of weighted samples $\{w^{(i,j)}_{k|k-1},\boldsymbol{x}^{(i,j)}_{k|k-1}\}_{j=1}^{L^{(i)}_{k|k-1}}$, i.e.,

$$p^{(i)}_{k|k-1}(\boldsymbol{x})=\sum_{j=1}^{L^{(i)}_{k|k-1}}w^{(i,j)}_{k|k-1}\delta(\boldsymbol{x}-\boldsymbol{x}^{(i,j)}_{k|k-1}), \tag{15}$$

the updated multi-target density

$$\pi_k=\{(r^{(i)}_{\mathrm{L},k},p^{(i)}_{\mathrm{L},k})\}_{i=1}^{M_{k|k-1}}\cup\{(r_{\mathrm{U},k}(\boldsymbol{z}),p_{\mathrm{U},k}(\cdot;\boldsymbol{z}))\}_{\boldsymbol{z}\in Z_k} \tag{16}$$

can be computed as follows:

The legacy tracks are

$$r^{(i)}_{\mathrm{L},k}=r^{(i)}_{k|k-1}\frac{1-\varrho^{(i)}_{\mathrm{L},k}}{1-r^{(i)}_{k|k-1}\varrho^{(i)}_{\mathrm{L},k}}, \tag{17}$$

$$p^{(i)}_{\mathrm{L},k}(\boldsymbol{x})=\sum_{j=1}^{L^{(i)}_{k|k-1}}w^{(i,j)}_{\mathrm{L},k}\delta(\boldsymbol{x}-\boldsymbol{x}^{(i,j)}_{k|k-1}), \tag{18}$$

where

$$\varrho^{(i)}_{\mathrm{L},k}=\sum_{j=1}^{L^{(i)}_{k|k-1}}w^{(i,j)}_{k|k-1}p_{\mathrm{D},k}(\boldsymbol{x}^{(i,j)}_{k|k-1}), \tag{19}$$

$$\tilde{w}^{(i,j)}_{\mathrm{L},k}=w^{(i,j)}_{k|k-1}(1-p_{\mathrm{D},k}(\boldsymbol{x}^{(i,j)}_{k|k-1})), \tag{20}$$

$$w^{(i,j)}_{\mathrm{L},k}=\frac{\tilde{w}^{(i,j)}_{\mathrm{L},k}}{\sum_{j=1}^{L^{(i)}_{k|k-1}}\tilde{w}^{(i,j)}_{\mathrm{L},k}}. \tag{21}$$

The measurement-updated tracks are

$$r_{\mathrm{U},k}(\boldsymbol{z})=\frac{\sum_{i=1}^{M_{k|k-1}}\frac{r^{(i)}_{k|k-1}(1-r^{(i)}_{k|k-1})\varrho^{(i)}_{\mathrm{U},k}(\boldsymbol{z})}{(1-r^{(i)}_{k|k-1}\varrho^{(i)}_{\mathrm{L},k})^2}}{\kappa_k(\boldsymbol{z})+\sum_{i=1}^{M_{k|k-1}}\frac{r^{(i)}_{k|k-1}\varrho^{(i)}_{\mathrm{U},k}(\boldsymbol{z})}{1-r^{(i)}_{k|k-1}\varrho^{(i)}_{\mathrm{L},k}}}, \tag{22}$$

$$p_{\mathrm{U},k}(\boldsymbol{x};\boldsymbol{z})=\sum_{i=1}^{M_{k|k-1}}\sum_{j=1}^{L^{(i)}_{k|k-1}}w^{(i,j)}_{\mathrm{U},k}(\boldsymbol{z})\delta(\boldsymbol{x}-\boldsymbol{x}^{(i,j)}_{k|k-1}), \tag{23}$$

where

$$\tilde{w}^{(i,j)}_{\mathrm{U},k}(\boldsymbol{z})=w^{(i,j)}_{k|k-1}\frac{r^{(i)}_{k|k-1}}{1-r^{(i)}_{k|k-1}}\psi_{k,z}(\boldsymbol{x}^{(i,j)}_{k|k-1}), \tag{24}$$

$$w^{(i,j)}_{\mathrm{U},k}(\boldsymbol{z})=\frac{\tilde{w}^{(i,j)}_{\mathrm{U},k}(\boldsymbol{z})}{\sum_{i=1}^{M_{k|k-1}}\sum_{j=1}^{L^{(i)}_{k|k-1}}\tilde{w}^{(i,j)}_{\mathrm{U},k}(\boldsymbol{z})}, \tag{25}$$

$$\varrho^{(i)}_{\mathrm{U},k}(\boldsymbol{z})=\sum_{j=1}^{L^{(i)}_{k|k-1}}w^{(i,j)}_{k|k-1}\psi_{k,z}(\boldsymbol{x}^{(i,j)}_{k|k-1}), \tag{26}$$

$$\psi_{k,z}(\boldsymbol{x}^{(i,j)}_{k|k-1})=g_k(\boldsymbol{z}|\boldsymbol{x}^{(i,j)}_{k|k-1})p_{\mathrm{D},k}(\boldsymbol{x}^{(i,j)}_{k|k-1}), \tag{27}$$

$g_k(\cdot|\boldsymbol{x}^{(i,j)}_{k|k-1})$ is the single target measurement likelihood at time k given predicted state $\boldsymbol{x}^{(i,j)}_{k|k-1}$, Z_k is the measurement set at time k, $p_{\mathrm{D},k}(\boldsymbol{x}^{(i,j)}_{k|k-1})$ is the

detection probability at time k given predicted state $\boldsymbol{x}_{k|k-1}^{(i,j)}$, and $\kappa_k(\cdot)$ is the clutter intensity at time k.

3. Resampling

For $i = 1, 2, \cdots, M_k$, set $L_k^{(i)} = r_k^{(i)} L_{\max}$, where $L_{\max}$ is the maximum number of particles for each hypothesized track and $M_k = M_{k|k-1} + |Z_k|$, where $|Z_k|$ is the number of measurements at time k. Resample $\left\{r_k^{(i)}, \{w_k^{(i,j)}, \boldsymbol{x}_k^{(i,j)}\}_{j=1}^{L_{k|k-1}^{(i)}}\right\}_{i=1}^{M_{k|k-1}} \cup \left\{r_k^{(i)}, \{w_k^{(i,j)}, \boldsymbol{x}_k^{(i,j)}\}_{j=1}^{L_{z,k}^{(i)}}\right\}_{i=1}^{|Z_k|}$ to obtain $\left\{r_k^{(i)}, \{w_k^{(i,j)}, \boldsymbol{x}_k^{(i,j)}\}_{j=1}^{L_k^{(i)}}\right\}_{i=1}^{M_k}$, where $L_{z,k}^{(i)}$ is the number of particles for the ith measurement-updated track.

2.2 Analysis of computing time

One cycle of SMC-MB recursion consists of three steps: prediction, update, and resampling. From Eq. (22) we can see that the computing time of SMC-MB recursion depends on both the number of particles and the number of measurements. Also, note that the computation of the existence probability consists of a series of complicated mathematical computations including multiplication, accumulation, and division in the update step, which increases the processing time. Fig. 1 shows the average computing time of 500 iterations of MC simulation of the prediction, update, and resampling for SMC-MB recursion versus varying clutter density (an average of 5–30 clutter measurements per scan), which will be detailed in Section 4.1. From Fig. 1, the prediction and resampling steps both consume much less time than the update step. Compared with the update step, the computing time in the prediction and resampling steps is almost negligible.

The filtering performance of the SMC-MB filter increases with the increases of the number of particles used to characterize each posterior hypothesized track density. However, the computing time increases as the number of particles increases. In practice, to achieve a tradeoff between filtering performance and computing time, an appropriate number of particles should be chosen for each hypothesized track. In this study the number of particles is chosen according to the suggestion given by Vo *et al.* (2009).

Also, note that the computing time in the update step grows linearly with the increase of the number of clutter measurements. Several measurements may be available at each time step, and each measurement may be generated by the survival target, the birth target, or the clutter. Specifically, in clutter environments, a lot of clutter measurements are contained. If all the measurements are considered in the update step, the computing time will increase significantly. Clutter measurements may also degrade the filtering performance. Therefore, most clutter measurements should be eliminated.

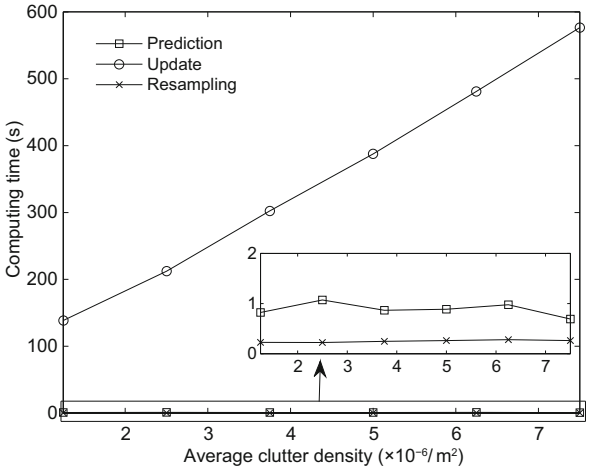

Fig. 1 Computing time of the SMC-MB filter versus varying clutter density

3 Measurement-driven SMC-MB filtering

3.1 Gating technique for the SMC-MB filter

Suppose the target motion dynamics and measurements for each target can be described as follows:

$$\boldsymbol{x}_k = f_k(\boldsymbol{x}_{k-1}) + \boldsymbol{w}_{k-1}, \tag{28}$$

$$\boldsymbol{z}_k = h_k(\boldsymbol{x}_k) + \boldsymbol{v}_k, \tag{29}$$

where $f_k(\cdot)$ and $h_k(\cdot)$ are known functions, which can be linear or nonlinear, and $\boldsymbol{w}_{k-1}$ and $\boldsymbol{v}_k$ are independent zero mean Gaussian process noise and measurement noise with known covariances $\boldsymbol{Q}_{k-1}$ and $\boldsymbol{R}_k$, respectively.

Gating has proven to be an effective method to eliminate clutter measurements in traditional target tracking (Blackman and Popoli, 1999). Therefore, we use the gating technique for the SMC-MB filter. The gating technique is designed for both survival and birth targets. Suppose at time k, the predicted

multi-target density for survival targets is

$$\pi_{\mathrm{P},k|k-1} = \left\{ r^{(i)}_{\mathrm{P},k|k-1}, \left\{ w^{(i,j)}_{\mathrm{P},k|k-1}, \boldsymbol{x}^{(i,j)}_{\mathrm{P},k|k-1} \right\}_{j=1}^{L^{(i)}_{k-1}} \right\}_{i=1}^{M_{k-1}}. \tag{30}$$

This means there are M_{k-1} hypothesized survival tracks at the prediction step. Gating should be designed for each hypothesized survival track. For the ith hypothesized survival track, the MC approximation of the predicted likelihood can be written as

$$\Lambda^{(i)}_{k|k-1} = \sum_{j=1}^{L^{(i)}_{k-1}} w^{(i,j)}_{\mathrm{P},k|k-1} \mathcal{N}(\boldsymbol{z}; h_k(\boldsymbol{x}^{(i,j)}_{\mathrm{P},k|k-1}), \boldsymbol{R}_k). \tag{31}$$

Note that Eq. (31) is a form of Gaussian mixture, which can be straightforwardly approximated by a single Gaussian distribution with mean and covariance given by

$$\bar{\boldsymbol{z}}^{(i)}_{\mathrm{P},k|k-1} = \sum_{j=1}^{L^{(i)}_{k-1}} w^{(i,j)}_{\mathrm{P},k|k-1} h_k(\boldsymbol{x}^{(i,j)}_{\mathrm{P},k|k-1}), \tag{32}$$

$$\begin{aligned} \boldsymbol{S}^{(i)}_{\mathrm{P},k|k-1} = \boldsymbol{R}_k + \sum_{j=1}^{L^{(i)}_{k-1}} \Big[& w^{(i,j)}_{\mathrm{P},k|k-1} \\ & \cdot \left(h_k(\boldsymbol{x}^{(i,j)}_{\mathrm{P},k|k-1}) - \bar{\boldsymbol{z}}^{(i)}_{\mathrm{P},k|k-1} \right) \\ & \cdot \left(h_k(\boldsymbol{x}^{(i,j)}_{\mathrm{P},k|k-1}) - \bar{\boldsymbol{z}}^{(i)}_{\mathrm{P},k|k-1} \right)^{\mathrm{T}} \Big]. \end{aligned} \tag{33}$$

The validation measurement set for survival targets is defined as $Z_{\mathrm{P},k}$ at time k, which can be obtained as follows:

$$\begin{aligned} Z_{\mathrm{P},k} = \Big\{ & \boldsymbol{z}_{k,s} : \left(\boldsymbol{z}_{k,s} - \bar{\boldsymbol{z}}^{(i)}_{\mathrm{P},k|k-1} \right)^{\mathrm{T}} \\ & \cdot \left(\boldsymbol{S}^{(i)}_{\mathrm{P},k|k-1} \right)^{-1} \left(\boldsymbol{z}_{k,s} - \bar{\boldsymbol{z}}^{(i)}_{\mathrm{P},k|k-1} \right) \le U_{\mathrm{P}} \Big\}_{\boldsymbol{z}_{k,s} \in Z_k}, \end{aligned} \tag{34}$$

where $\boldsymbol{z}_{k,s}$ is the sth measurement, and U_{P} is the gating threshold for survival targets. The choice of the gating threshold is important. If the gating threshold is too small, the true measurements may not fall into the validation region. As the gating threshold increases, the probability of achieving true measurements in the validation region increases. Meanwhile, the probability of obtaining clutter measurements in the validation region increases. The gating threshold can be computed according to (Blackman and Popoli, 1999)

$$U = -2\ln(1 - P_{\mathrm{g}}) \tag{35}$$

for 2D measurements, where P_{g} is the probability that a target-generated measurement falls into the validation region. For higher dimensional measurements, readers can refer to Blackman and Popoli (1999) for details.

Through the above steps, the survival measurement set is obtained, and the residual measurement set is described as follows:

$$\tilde{Z}_k = Z_k - Z_{\mathrm{P},k}, \tag{36}$$

where $\tilde{Z}_k$ denotes the residual measurement set at time k. The residual measurement set consists of the birth and clutter measurements. If no birth target appears, the residual measurement set consists of only clutter measurements.

Here, we use an example to illustrate the gating technique for survival targets (Fig. 2). The key of the proposed approach can be described as follows. If the validation region of the ith hypothesized track is denoted as $\Omega_{\mathrm{g}}(i)$, then the total validation region is the union of the validation regions for all hypothesized tracks, which can be expressed as follows:

$$\Omega_{\mathrm{g}} = \Omega_{\mathrm{g}}(1) \cup \Omega_{\mathrm{g}}(2) \cup \Omega_{\mathrm{g}}(3). \tag{37}$$

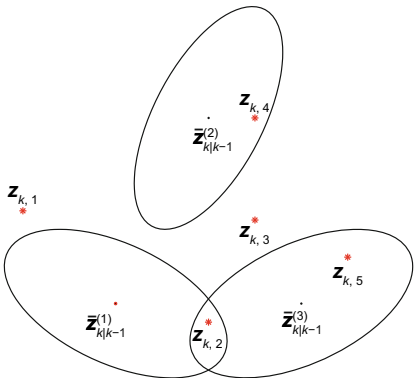

Fig. 2 Illustration of the gating technique for the SMC-MB filter ('·' denotes the mean of the predicted measurements for each hypothesized track, the ellipse denotes the validation region for each hypothesized track, and '∗' denotes the measurements at time k)

If the measurements fall into the union validation region, they are validation measurements; otherwise, they are residual measurements. In this example (Fig. 2), we can see that $\boldsymbol{z}_{k,2}$, $\boldsymbol{z}_{k,4}$, and $\boldsymbol{z}_{k,5}$ are validation measurements, and $\boldsymbol{z}_{k,1}$ and $\boldsymbol{z}_{k,3}$ are residual measurements.

Although the survival measurements can be obtained through the above steps, the birth measurements may not be contained. To obtain the birth

measurements from the residual measurement set, the gating technique is used again for spontaneous targets. The validation measurement set for birth targets is denoted as $Z_{\Gamma,k}$ at time k, which can be obtained as follows:

$$Z_{\Gamma,k}=\Big\{\tilde{\boldsymbol{z}}_{k,s}:\big(\tilde{\boldsymbol{z}}_{k,s}-\bar{\boldsymbol{z}}_{\Gamma,k}^{(i)}\big)^{\mathrm{T}}\cdot\big(\boldsymbol{S}_{\Gamma,k}^{(i)}\big)^{-1}\big(\tilde{\boldsymbol{z}}_{k,s}-\bar{\boldsymbol{z}}_{\Gamma,k}^{(i)}\big)\le U_{\Gamma}\Big\}_{\tilde{\boldsymbol{z}}_{k,s}\in\tilde{Z}_k},\tag{38}$$

where

$$\bar{z}_{\Gamma,k}^{(i)}=\sum_{j=1}^{L_{\Gamma,k}^{(i)}}w_{\Gamma,k}^{(i,j)}h_k(\boldsymbol{x}_{\Gamma,k}^{(i,j)}),\tag{39}$$

$$\boldsymbol{S}_{\Gamma,k}^{(i)}=\boldsymbol{R}_k+\sum_{j=1}^{L_{\Gamma,k}^{(i)}}w_{\Gamma,k}^{(i,j)}\big(h_k(\boldsymbol{x}_{\Gamma,k}^{(i,j)})-\bar{\boldsymbol{z}}_{\Gamma,k}^{(i)}\big)\big(h_k(\boldsymbol{x}_{\Gamma,k}^{(i,j)})-\bar{\boldsymbol{z}}_{\Gamma,k}^{(i)}\big)^{\mathrm{T}},\tag{40}$$

$\tilde{\boldsymbol{z}}_{k,s}$ is the sth measurement and U_Γ is the gating threshold for birth targets, which can be calculated according to Eq. (35).

Finally, the survival and birth measurements can be distinguished from the original measurements. Algorithms 1 and 2 present the pseudo-code of the gating technique for survival and birth targets, respectively.

Algorithm 1 Gating technique for survival targets

for $i=1,\cdots,M_{k-1}$ **do**
  for $j=1,\cdots,L_{k-1}^{(i)}$ **do**
    sample $\boldsymbol{x}_{k|k-1}^{(i,j)}\sim q_k^{(i)}(\cdot|\boldsymbol{x}_{k-1}^{(i,j)},Z_k)$;
    $w_{k|k-1}^{(i,j)}=\frac{w_{k-1}^{(i,j)}f_{k|k-1}(\boldsymbol{x}_{k|k-1}^{(i,j)}|\boldsymbol{x}_{k-1}^{(i,j)})p_{\mathrm{S},k}(\boldsymbol{x}_{k-1}^{(i,j)})}{q_k^{(i)}(\boldsymbol{x}_{k|k-1}^{(i,j)}|\boldsymbol{x}_{k-1}^{(i,j)},Z_k)}$;
  end for
end for
$r_{k|k-1}^{(i)}=r_{k-1}^{(i)}\sum_{j=1}^{L_{k-1}^{(i)}}w_{k-1}^{(i,j)}p_{\mathrm{S},k}(\boldsymbol{x}_{k-1}^{(i,j)})$;
$w_{k|k-1}^{(i,j)}=\frac{w_{k|k-1}^{(i,j)}}{\sum_{j=1}^{L_{k-1}^{(i)}}w_{k|k-1}^{(i,j)}}$;
$L_{k|k-1}^{(i)}=L_{k-1}^{(i)}$;
$\bar{\boldsymbol{z}}_{k|k-1}^{(i)}=\sum_{j=1}^{L_{k-1}^{(i)}}w_{k|k-1}^{(i,j)}h_k(\boldsymbol{x}_{k|k-1}^{(i,j)})$;
$\boldsymbol{S}_{k|k-1}^{(i)}=\boldsymbol{R}_k+\sum_{j=1}^{L_{k-1}^{(i)}}w_{k|k-1}^{(i,j)}\big(h_k(\boldsymbol{x}_{k|k-1}^{(i,j)})-\bar{\boldsymbol{z}}_{k|k-1}^{(i)}\big)\cdot\big(h_k(\boldsymbol{x}_{k|k-1}^{(i,j)})-\bar{\boldsymbol{z}}_{k|k-1}^{(i)}\big)^{\mathrm{T}}$;
set $Z_{\mathrm{P},k}=\varnothing$;
set flag $=0$;
for $\boldsymbol{z}\in Z_k$ **do**
  for $i=1,\cdots,M_{k-1}$ **do**
    if $\big(\boldsymbol{z}-\bar{\boldsymbol{z}}_{k|k-1}^{(i)}\big)^{\mathrm{T}}\big(\boldsymbol{S}_{k|k-1}^{(i)}\big)^{-1}\big(\boldsymbol{z}-\bar{\boldsymbol{z}}_{k|k-1}^{(i)}\big)\le U_{\mathrm{P}}$ **then**
      $Z_{\mathrm{P},k}=[Z_{\mathrm{P},k},\boldsymbol{z}]$;
      flag $=1$;
      break;
    end if
    if flag $==1$ **then**
      break;
    end if
  end for
end for
$\tilde{Z}_k=Z_k-Z_{\mathrm{P},k}$;

3.2 Measurement-driven approach

In this study, we propose a measurement-driven approach for the SMC-MB filter. Since the survival and birth measurements are distinguished from the original measurements using the gating technique, the survival measurement set is used to update both survival and birth targets, and the birth measurement set is used to update only birth targets. We call this method the measurement-driven approach. Algorithm 3 gives the pseudo-code for the measurement-driven approach.

Remark 1 Note that the survival measurement set cannot be used to update only survival targets. It can be explained as follows: If the location of the birth target is close to the predicted location of survival targets, then the validation survival measurements may contain the birth measurements, and the residual measurement set may not contain birth measurements, so birth measurements cannot be obtained from the residual measurement set. Using the measurements containing birth measurements to update only survival targets may cause the loss of birth targets.

3.3 Comparison of the cycle index in the update step

For SMC-MB recursion, all the measurements in the set Z_k are considered to update both survival and birth targets in the update step. For the proposed approach, the survival measurements are used to update both survival and birth targets, and the birth measurements are used to update only the birth targets in the update step. For the proposed approach, the processing time of survival targets depends on the number of survival measurements, the number of survival particles, and the number of birth particles, and the processing time of birth targets depends only on the number of birth measurements

Algorithm 2 Gating technique for birth targets

for $i = M_{k-1}+1, \cdots, M_{k-1}+M_{\Gamma,k}$ **do**
  for $j = 1, \cdots, L_{\Gamma,k}^{(i-M_{k-1})}$ **do**
    sample $\boldsymbol{x}_{k|k-1}^{(i,j)} \sim b_k^{(i)}(\cdot|Z_k)$;
    $w_{k|k-1}^{(i,j)} = \dfrac{p_{\Gamma,k}(\boldsymbol{x}_{k|k-1}^{(i,j)})}{b_k^{(i)}(\boldsymbol{x}_{k|k-1}^{(i,j)}|Z_k)}$;
  end for
end for
$r_{k|k-1}^{(i)} = r_{\Gamma,k}^{(i-M_{k-1})}$;
$w_{k|k-1}^{(i,j)} = \dfrac{w_{k|k-1}^{(i,j)}}{\sum_{j=1}^{L_{\Gamma,k}^{(i-M_{k-1})}} w_{k|k-1}^{(i,j)}}$;
$L_{k|k-1}^{(i)} = L_{\Gamma,k}^{(i-M_{k-1})}$;
$M_{k|k-1} = M_{k-1} + M_{\Gamma,k}$;
$\bar{\boldsymbol{z}}_{k|k-1}^{(i)} = \sum_{j=1}^{L_{k|k-1}^{(i)}} w_{k|k-1}^{(i,j)} h_k(\boldsymbol{x}_{k|k-1}^{(i,j)})$;
$\boldsymbol{S}_{k|k-1}^{(i)} = \boldsymbol{R}_k + \sum_{j=1}^{L_{k|k-1}^{(i)}} w_{k|k-1}^{(i,j)} \cdot \big(h_k(\boldsymbol{x}_{k|k-1}^{(i,j)}) - \bar{\boldsymbol{z}}_{k|k-1}^{(i)}\big)\big(h_k(\boldsymbol{x}_{k|k-1}^{(i,j)}) - \bar{\boldsymbol{z}}_{k|k-1}^{(i)}\big)^{\mathrm{T}}$;
set $Z_{\Gamma,k} = \varnothing$;
set flag = 0;
for $\boldsymbol{z} \in \tilde{Z}_k$ **do**
  for $i = M_{k-1}+1, \cdots, M_{k|k-1}$ **do**
    if $\big(\boldsymbol{z} - \bar{\boldsymbol{z}}_{k|k-1}^{(i)}\big)^{\mathrm{T}} \big(\boldsymbol{S}_{k|k-1}^{(i)}\big)^{-1} \big(\boldsymbol{z} - \bar{\boldsymbol{z}}_{k|k-1}^{(i)}\big) \le U_\Gamma$ **then**
      $Z_{\Gamma,k} = [Z_{\Gamma,k}, \boldsymbol{z}]$;
      flag = 1;
      break;
    end if
    if flag==1 **then**
      break;
    end if
  end for
end for

and the number of birth particles. According to the above analysis, the cycle index of SMC-MB recursion in the update step is $|Z_k|(\sum_{i=1}^{M_{k-1}} L_{k-1}^{(i)} + \sum_{i=1}^{M_{\Gamma,k}} L_{\Gamma,k}^{(i)})$, and the cycle index of the proposed approach is $|Z_{\mathrm{P},k}|(\sum_{i=1}^{M_{k-1}} L_{k-1}^{(i)} + \sum_{i=1}^{M_{\Gamma,k}} L_{\Gamma,k}^{(i)}) + |Z_{\Gamma,k}| \sum_{i=1}^{M_{\Gamma,k}} L_{\Gamma,k}^{(i)}$. In clutter environments, $|Z_k| > |Z_{\mathrm{P},k}| + |Z_{\Gamma,k}|$; thus, $|Z_k|(\sum_{i=1}^{M_{k-1}} L_{k-1}^{(i)} + \sum_{i=1}^{M_{\Gamma,k}} L_{\Gamma,k}^{(i)}) > |Z_{P,k}|(\sum_{i=1}^{M_{k-1}} L_{k-1}^{(i)} + \sum_{i=1}^{M_{\Gamma,k}} L_{\Gamma,k}^{(i)}) + |Z_{\Gamma,k}| \sum_{i=1}^{M_{\Gamma,k}} L_{\Gamma,k}^{(i)}$. According to the above analysis, the proposed approach will consume less time than the SMC-MB filter in the update step.

Algorithm 3 Measurement-driven algorithm

Step 1: Update for survival targets
for each $\boldsymbol{z} \in Z_{\mathrm{P},k}$ **do**
  set $l = 0$;
  for $i = 1, \cdots, M_{k|k-1}$ **do**
    for $j = 1, \cdots, L_{k|k-1}^{(i)}$ **do**
      $l = l + 1$;
      $\psi_{k,\boldsymbol{z}}^{(i,j)} = g_k(\boldsymbol{z}|\boldsymbol{x}_{k|k-1}^{(i,j)}) P_{\mathrm{D},k}(\boldsymbol{x}_{k|k-1}^{(i,j)})$;
      $w_{\mathrm{U},k}^{(i,j)}(\boldsymbol{z}) = w_{k|k-1}^{(i,j)} \dfrac{r_{k|k-1}^{(i,j)}}{1 - r_{k|k-1}^{(i,j)}} \psi_{k,\boldsymbol{z}}^{(i,j)}$;
    end for
    $\varrho_{\mathrm{U},k}^{(i)}(\boldsymbol{z}) = \sum_{j=1}^{L_{k|k-1}^{(i)}} w_{k|k-1}^{(i,j)} \psi_{k,\boldsymbol{z}}^{(i,j)}$;
    $\varrho_{\mathrm{L},k}^{(i)} = \sum_{j=1}^{L_{k|k-1}^{(i)}} w_{k|k-1}^{(i,j)} p_{\mathrm{D},k}(\boldsymbol{x}_{k|k-1}^{(i,j)})$;
  end for
  $L_k(\boldsymbol{z}) = l$;
  $w_{\mathrm{U},k}^{(i,j)}(\boldsymbol{z}) = \dfrac{w_{\mathrm{U},k}^{(i,j)}(\boldsymbol{z})}{\sum_{i=1}^{M_{k|k-1}} \sum_{j=1}^{L_{k|k-1}^{(i)}} w_{\mathrm{U},k}^{(i,j)}(\boldsymbol{z})}$;
  $r_k(\boldsymbol{z}) = \dfrac{\sum_{i=1}^{M_{k|k-1}} \dfrac{r_{k|k-1}^{(i)}(1 - r_{k|k-1}^{(i)}) \varrho_{\mathrm{U},k}^{(i)}(\boldsymbol{z})}{(1 - r_{k|k-1}^{(i)} \varrho_{\mathrm{L},k}^{(i)})^2}}{\kappa_k(\boldsymbol{z}) + \sum_{i=1}^{M_{k|k-1}} \dfrac{r_{k|k-1}^{(i)} \varrho_{\mathrm{U},k}^{(i)}(\boldsymbol{z})}{1 - r_{k|k-1}^{(i)} \varrho_{\mathrm{L},k}^{(i)}}}$;
end for
Step 2: Update for birth targets
for each $\boldsymbol{z} \in Z_{\Gamma,k}$ **do**
  set $l = 0$;
  for $i = M_{k-1}+1, \cdots, M_{k|k-1}$ **do**
    for $j = 1, \cdots, L_{k|k-1}^{(i)}$ **do**
      $l = l + 1$;
      $\psi_{k,\boldsymbol{z}}^{(i,j)} = g_k(\boldsymbol{z}|\boldsymbol{x}_{k|k-1}^{(i,j)}) P_{\mathrm{D},k}(\boldsymbol{x}_{k|k-1}^{(i,j)})$;
      $w_{\mathrm{U},k}^{(i,j)}(\boldsymbol{z}) = w_{k|k-1}^{(i,j)} \dfrac{r_{k|k-1}^{(i,j)}}{1 - r_{k|k-1}^{(i,j)}} \psi_{k,\boldsymbol{z}}^{(i,j)}$;
    end for
    $\varrho_{\mathrm{U},k}^{(i)}(\boldsymbol{z}) = \sum_{j=1}^{L_{k|k-1}^{(i)}} w_{k|k-1}^{(i,j)} \psi_{k,\boldsymbol{z}}^{(i,j)}$;
    $\varrho_{\mathrm{L},k}^{(i)} = \sum_{j=1}^{L_{k|k-1}^{(i)}} w_{k|k-1}^{(i,j)} p_{\mathrm{D},k}(\boldsymbol{x}_{k|k-1}^{(i,j)})$;
  end for
  $L_k(\boldsymbol{z}) = l$;
  $w_{\mathrm{U},k}^{(i,j)}(\boldsymbol{z}) = \dfrac{w_{\mathrm{U},k}^{(i,j)}(\boldsymbol{z})}{\sum_{i=M_{k-1}}^{M_{k|k-1}} \sum_{j=1}^{L_{k|k-1}^{(i)}} w_{\mathrm{U},k}^{(i,j)}(\boldsymbol{z})}$;
  $r_k(\boldsymbol{z}) = \dfrac{\sum_{i=M_{k-1}}^{M_{k|k-1}} \dfrac{r_{k|k-1}^{(i)}(1 - r_{k|k-1}^{(i)}) \varrho_{\mathrm{U},k}^{(i)}(\boldsymbol{z})}{(1 - r_{k|k-1}^{(i)} \varrho_{\mathrm{L},k}^{(i)})^2}}{\kappa_k(\boldsymbol{z}) + \sum_{i=M_{k-1}}^{M_{k|k-1}} \dfrac{r_{k|k-1}^{(i)} \varrho_{\mathrm{U},k}^{(i)}(\boldsymbol{z})}{1 - r_{k|k-1}^{(i)} \varrho_{\mathrm{L},k}^{(i)}}}$;
end for
$M_k = M_{k|k-1} + |Z_{\mathrm{P},k}| + |Z_{\Gamma,k}|$;

4 Simulation results

4.1 Simulation for a linear Gaussian example

Suppose the target motion dynamics is linear, described as

$$\boldsymbol{x}_k = \boldsymbol{F}_k \boldsymbol{x}_{k-1} + \boldsymbol{w}_{k-1}, \tag{41}$$

where process noise $\boldsymbol{w}_{k-1}$ is a zero mean Gaussian noise with known covariance $\boldsymbol{Q}_{k-1}$, and target state $\boldsymbol{x}_k = [p_{x,k}, \dot{p}_{x,k}, p_{y,k}, \dot{p}_{y,k}]^{\mathrm{T}}$ at time k consists of position component $(p_{x,k}, p_{y,k})$ and velocity component $(\dot{p}_{x,k}, \dot{p}_{y,k})$. The target transition matrix and process noise are specified by (Bar-Shalom *et al.*, 2001)

$$\boldsymbol{F}_k = \begin{bmatrix} 1 & T & 0 & 0 \\ 0 & 1 & 0 & 0 \\ 0 & 0 & 1 & T \\ 0 & 0 & 0 & 1 \end{bmatrix}, \tag{42}$$

$$\boldsymbol{Q}_{k-1} = \sigma_{\mathrm{w}}^2 \begin{bmatrix} T^3/3 & T^2/2 & 0 & 0 \\ T^2/2 & T & 0 & 0 \\ 0 & 0 & T^3/3 & T^2/2 \\ 0 & 0 & T^2/2 & T \end{bmatrix}, \tag{43}$$

where T is the sampling period, and σ_{w} is the standard deviation of the process noise.

The target measurement model is also linear, described as

$$\boldsymbol{z}_k = \boldsymbol{H}_k \boldsymbol{x}_k + \boldsymbol{v}_k, \tag{44}$$

where

$$\boldsymbol{H}_k = \begin{bmatrix} 1 & 0 & 0 & 0 \\ 0 & 0 & 1 & 0 \end{bmatrix}, \tag{45}$$

the measurement noise $\boldsymbol{v}_k$ is a zero-mean Gaussian noise with known covariance

$$\boldsymbol{R} = \sigma_{\mathrm{v}}^2 \begin{bmatrix} 1 & 0 \\ 0 & 1 \end{bmatrix}, \tag{46}$$

and σ_{v} is the standard deviation of the measurement noise.

4.1.1 Simulation scenario

Consider a 2D scenario with a time-varying number of targets observed in clutter environments. The surveillance region is $[-1000, 1000]$ m $\times$ $[-1000, 1000]$ m. A maximum of five targets appear on the scenario, and targets appear and terminate randomly. The true trajectories of the targets are shown in Fig. 3.

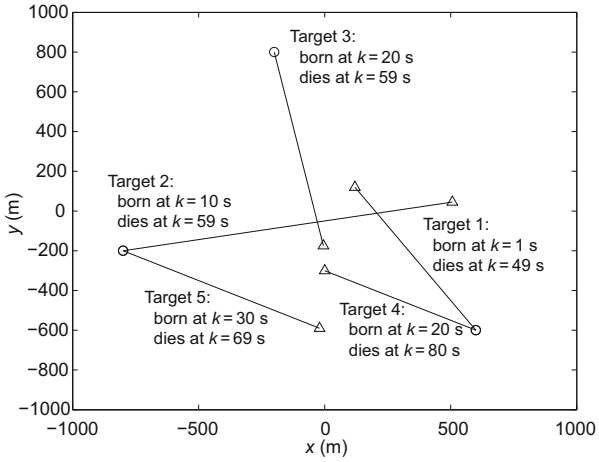

Fig. 3 True target tracks in the xOy plane (the start and end positions for each track are denoted by ○ and △, respectively)

The birth process is modeled as an MB-RFS (Vo *et al.*, 2009), which can be described as follows: $\pi_\Gamma = \{(r_\Gamma^{(i)}, p_\Gamma^{(i)})\}_{i=1}^3$, where $r_\Gamma^{(i)} = 0.03$, $p_\Gamma^{(i)} = \mathcal{N}(\boldsymbol{x}; \boldsymbol{m}_\Gamma^{(i)}, \boldsymbol{P}_\Gamma^{(i)})$, $\boldsymbol{m}_\Gamma^{(1)} = [600, 0, -600, 0]^{\mathrm{T}}$, $\boldsymbol{m}_\Gamma^{(2)} = [-800, 0, -200, 0]^{\mathrm{T}}$, $\boldsymbol{m}_\Gamma^{(3)} = [-200, 0, 800, 0]^{\mathrm{T}}$, and $\boldsymbol{P}_\Gamma^{(1)} = \boldsymbol{P}_\Gamma^{(2)} = \boldsymbol{P}_\Gamma^{(3)} = \mathrm{diag}\{10, 10, 10, 10\}^2$.

Clutter is modeled as a Poisson RFS K_k with intensity (Vo and Ma, 2006)

$$\kappa_k = \lambda_{\mathrm{c}} V u(\boldsymbol{z}), \tag{47}$$

where λ_{c} is the average number of clutter measurements per scan, and $u(\boldsymbol{z})$ is the uniform density over the surveillance region.

At each time step, a maximum of $L_{\max} = 1000$ and minimum of $L_{\min} = 300$ particles are imposed for each hypothesized track, and hypothesized tracks are pruned with a threshold of $T_{\mathrm{r}} = 10^{-4}$ and a maximum of 100 tracks. The survival probability is $P_{\mathrm{S},k} = 0.99$, the detection probability is $p_{\mathrm{D},k} = 0.98$, the sampling period is $T = 1$ s, the standard deviation of the process noise is $\sigma_{\mathrm{w}} = 10$ m/s^2, and the standard deviation of the measurement noise is $\sigma_{\mathrm{v}} = 10$ m. P_{g} is 0.999 for both survival and birth targets.

4.1.2 Metrics for multi-target filtering

We use the optimal sub-pattern assignment (OSPA) as a multi-target miss-distance metric as suggested by Schuhmacher *et al.* (2008), as it can jointly capture the differences in cardinality and individual elements between two finite sets. The OSPA metric $\bar{d}_p^{(c)}$ is defined as follows. Let $d^{(c)}(\boldsymbol{x}, \boldsymbol{y}) :=$

$\min(c, ||\boldsymbol{x}-\boldsymbol{y}||)$ denote the distance between $\boldsymbol{x}, \boldsymbol{y}$ cut off at $c > 0$, and Π_k the set of permutations on $\{1, 2, \cdots, k\}$, where $||\cdot||$ denotes the 2-norm. For $1 \leq p \leq \infty$, $c > 0$, and arbitrary finite subsets $X = \{\boldsymbol{x}_1, \boldsymbol{x}_2, \cdots, \boldsymbol{x}_m\}$ and $Y = \{\boldsymbol{y}_1, \boldsymbol{y}_2, \cdots, \boldsymbol{y}_n\}$, where $m, n \in \{0, 1, 2, \cdots\}$, define

$$\bar{d}_p^{(c)}(X,Y) \begin{cases} := \left[\frac{1}{n}\left(\min\limits_{\pi\in\Pi_n}\sum\limits_{i=1}^{m} d^{(c)}(\boldsymbol{x}_i, \boldsymbol{y}_{\pi_{(i)}})^p + c^p(n-m)\right)\right]^{\frac{1}{p}}, & \\ & m \leq n, \\ = \bar{d}_p^{(c)}(Y,X), & m > n, \\ = 0, & m = n = 0. \end{cases} \tag{48}$$

The order parameter p determines the sensitivity to outliers, and the cut-off parameter c determines the relative weighting of the penalties assigned to cardinality and localization errors.

4.1.3 Monte Carlo runs

To verify the real-time performance and filtering performance of the proposed approach, 500 MC trials are performed on the same target tracks but with randomly generated measurement data. For comparison, 500 MC trials are also performed on exactly the same data using the SMC-MB filter. The clutter density is $\lambda_c = 2.5 \times 10^{-6}/\mathrm{m}^2$ (an average of 10 clutter measurements per can).

Fig. 4 plots the true tracks, measurements, and estimates in x and y directions versus time for the proposed approach. From Fig. 4, the proposed approach is also able to track the targets correctly. Fig. 5 shows the mean and standard deviation of the cardinality statistics versus time for the SMC-MB filter and the proposed approach. It is shown that the cardinality statistics for both the SMC-MB filter and the proposed approach converges to the true value, and that the standard derivation of the proposed approach is similar to that of the SMC-MB filter. Fig. 6 shows the average OSPA distance (when $p = 2$ and $c = 200$) versus time for both approaches. The curves of these two approaches almost totally overlap. This indicates that the filtering performance of the proposed approach is almost the same as that of the SMC-MB filter.

Table 1 gives the time averaged OSPA distance and computing time of 500 MC runs in MATLAB

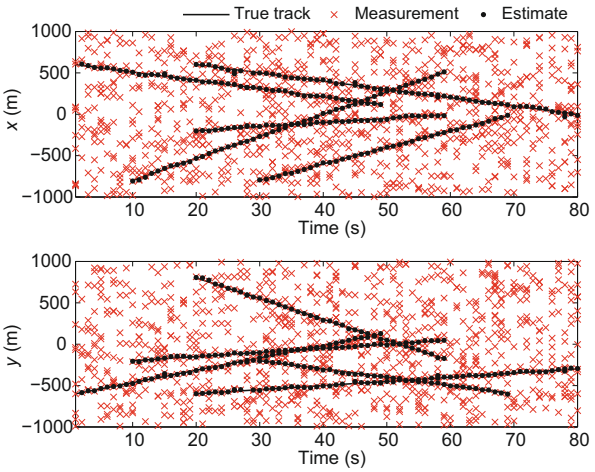

Fig. 4 True target tracks, measurements, and estimates in x and y directions versus time for the proposed approach

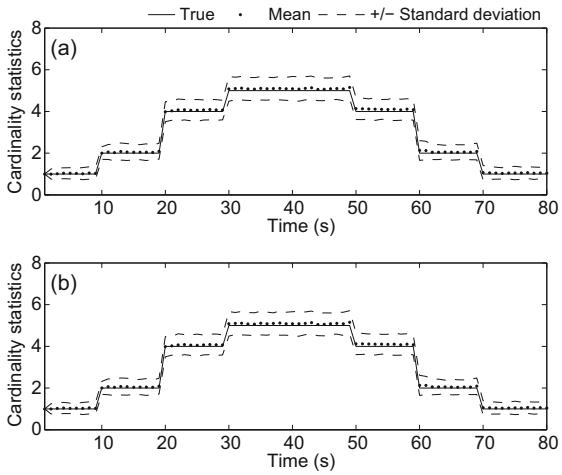

Fig. 5 The average of cardinality statistics of 500 Monte Carlo runs versus time for the SMC-MB filter (a) and the proposed approach (b)

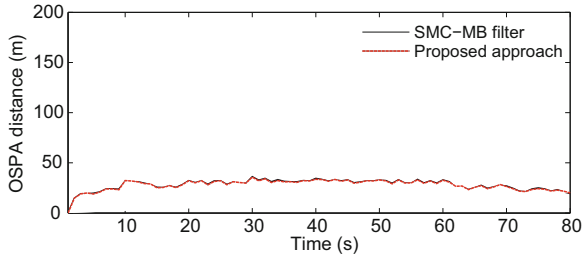

Fig. 6 The average OSPA distance for both approaches (p=2, c=200)

R2011a on a laptop with clutter density $\lambda_c = 2.5 \times 10^{-6}/\mathrm{m}^2$. The time averaged OSPA distance of the proposed approach is almost the same as that of the SMC-MB filter. Compared with the SMC-MB filter, the proposed approach has a much higher processing

speed. The reason is that the proposed approach discards most clutter measurements.

To further verify the effectiveness of the proposed approach, 500 MC trials are performed for both approaches over a varying clutter density from $1.25 \times 10^{-6}/\mathrm{m}^2$ to $7.50 \times 10^{-6}/\mathrm{m}^2$ (an average of 5–30 clutter measurements per scan). Fig. 7 shows that the time averaged OSPA distance of the proposed approach is similar to that of the SMC-MB filter under different clutter densities, but that the proposed approach consumes less computing time.

Table 1 Comparison between the SMC-MB filter and the proposed approach for the linear example

Filtering algorithm	Time averaged OSPA distance (m)	Average computing time (s)
SMC-MB filter	27.95	213.59
Proposed approach	27.90	76.09

The real-time performance improvement (RTPI) (Zheng *et al.*, 2013) is used to evaluate the real-time performance, defined as

$$\mathrm{RTPI} = \frac{t_\mathrm{S} - t_\mathrm{P}}{t_\mathrm{S}} \times 100\%, \tag{49}$$

where t_S and t_P are the MC average computing time for the SMC-MB filter and the proposed approach, respectively. Fig. 8 plots the RTPI for the proposed approach versus varying clutter density. It can be seen that the proposed approach gains more improvement when clutter density increases.

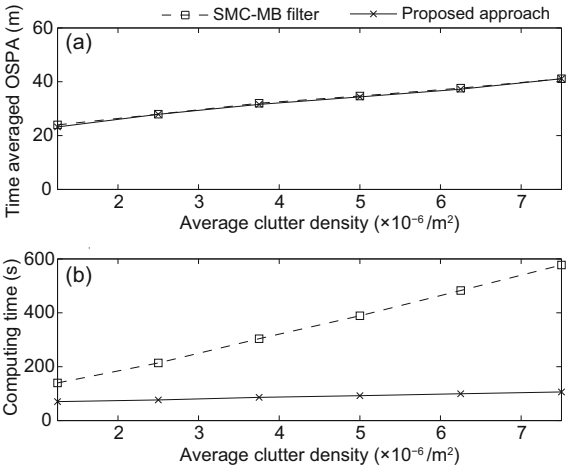

Fig. 7 Time averaged OSPA distance (a) and average computing time (b) versus varying clutter density

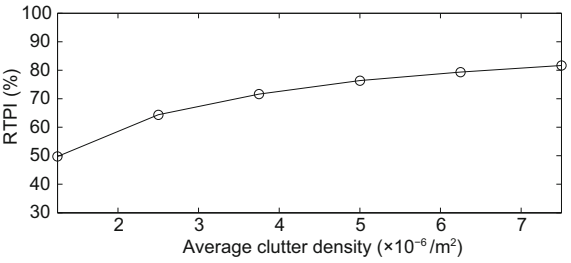

Fig. 8 Real-time performance improvement (RTPI) versus varying clutter density

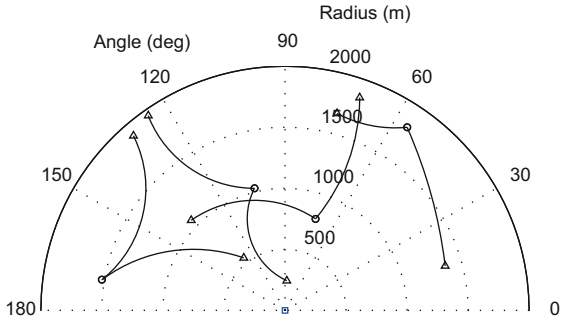

Fig. 9 True target tracks in the $r\theta$ plane (the start and end positions for each track are denoted by ○ and △ respectively, and the sensor is denoted by □)

4.2 Simulation for a nonlinear example

In this subsection a nonlinear example is used to verify the effectiveness of the proposed approach.

4.2.1 Simulation scenario

Consider the noisy bearings and range measurements with a varying number of targets observed in clutter environments. The surveillance region size is $[0, \pi]$ rad $\times$ $[0, 2000]$ m. A maximum of eight targets appear on the scenario, and targets appear and terminate randomly. The true tracks are shown in Fig. 9.

The motion dynamics is a coordinated turn (CT) model, which is described as (Bar-Shalom *et al.*, 2001; Li and Jilkov, 2003)

$$\boldsymbol{x}_k = \boldsymbol{F}(\omega_{k-1})\boldsymbol{x}_{k-1} + \boldsymbol{G}\boldsymbol{w}_{k-1}, \tag{50}$$

where

$$\boldsymbol{F}(\omega_{k-1}) = \begin{bmatrix} 1 & \frac{\sin(\omega_{k-1}T)}{\omega_{k-1}} & 0 & -\frac{1-\cos(\omega_{k-1}T)}{\omega_{k-1}} & 0 \\ 0 & \cos(\omega_{k-1}T) & 0 & -\sin(\omega_{k-1}T) & 0 \\ 0 & \frac{1-\cos(\omega_{k-1}T)}{\omega_{k-1}} & 1 & \frac{\sin(\omega_{k-1}T)}{\omega_{k-1}} & 0 \\ 0 & \sin(\omega_{k-1}T) & 0 & \cos(\omega_{k-1}T) & 0 \\ 0 & 0 & 0 & 0 & 1 \end{bmatrix}, \tag{51}$$

$$\boldsymbol{G}=\begin{bmatrix} T^2/2 & 0 & 0 \\ T & 0 & 0 \\ 0 & T^2/2 & 0 \\ 0 & T & 0 \\ 0 & 0 & T \end{bmatrix}, \tag{52}$$

$T=1$ s, $\boldsymbol{w}_{k-1}\sim\mathcal{N}(\cdot;0,\boldsymbol{Q}_{k-1})$, the process noise covariance is $\boldsymbol{Q}_{k-1}=\mathrm{diag}\{\sigma_{\mathrm{w}}^2,\sigma_{\mathrm{w}}^2,\sigma_{\omega}^2\}$, $\sigma_{\mathrm{w}}=5$ m/s^2, and $\sigma_{\omega}=\pi/180$ rad/s. The target state $\boldsymbol{x}_k=[p_{x,k},\dot{p}_{x,k},p_{y,k},\dot{p}_{y,k},\omega_k]^{\mathrm{T}}$ consists of position component $(p_{x,k},p_{y,k})$, velocity component $(\dot{p}_{x,k},\dot{p}_{y,k})$, and turn rate ω_k.

The measurement model is a noisy bearing and range vector, described as follows:

$$\boldsymbol{z}_k=\begin{bmatrix} \arctan\left(\dfrac{p_{x,k}-p_{\mathrm{Se},x}}{p_{y,k}-p_{\mathrm{Se},y}}\right) \\ \sqrt{(p_{x,k}-p_{\mathrm{Se},x})^2+(p_{y,k}-p_{\mathrm{Se},y})^2} \end{bmatrix}+\boldsymbol{v}_k, \tag{53}$$

where $(p_{\mathrm{Se},x},p_{\mathrm{Se},y})=(0,0)$ is the sensor position, the measurement noise $\boldsymbol{v}_k\sim\mathcal{N}(\cdot;0,\boldsymbol{R}_k)$ with $\boldsymbol{R}_k=\mathrm{diag}\{\sigma_\theta^2,\sigma_r^2\}$, $\sigma_\theta=1\times(\pi/180)$ rad/s, and $\sigma_r=5$ m. The birth process is an MB-RFS with density $\pi_\Gamma=\{(r_\Gamma^{(i)},p_\Gamma^{(i)})\}_{i=1}^4$, where $r_\Gamma^{(1)}=r_\Gamma^{(2)}=r_\Gamma^{(3)}=r_\Gamma^{(4)}=0.03$, $p_\Gamma^{(i)}=\mathcal{N}(\boldsymbol{x};\boldsymbol{m}_\Gamma^{(i)},\boldsymbol{P}_\Gamma^{(i)})$, $\boldsymbol{m}_\Gamma^{(1)}=[-1500,0,250,0,0]^{\mathrm{T}}$, $\boldsymbol{m}_\Gamma^{(2)}=[-250,0,1000,0,0]^{\mathrm{T}}$, $\boldsymbol{m}_\Gamma^{(3)}=[250,0,750,0,0]^{\mathrm{T}}$, $\boldsymbol{m}_\Gamma^{(4)}=[1000,0,1500,0,0]^{\mathrm{T}}$, and $\boldsymbol{P}_\Gamma^{(1)}=\boldsymbol{P}_\Gamma^{(2)}=\boldsymbol{P}_\Gamma^{(3)}=\boldsymbol{P}_\Gamma^{(4)}=\mathrm{diag}\{10,10,10,10,1\times(\pi/180)\}^2$. The survival probability is $P_{\mathrm{S},k}=0.99$. The detection probability is $p_{\mathrm{D},k}=0.98$. Clutter is a Poisson RFS with density $\lambda_{\mathrm{c}}=1.6\times10^{-3}/(\mathrm{rad}\cdot\mathrm{m})$ (an average of 10 clutter measurements per scan).

4.2.2 Monte Carlo runs

To compare the proposed approach with the SMC-MB filter for the nonlinear example, 500 MC trials are performed on the same target tracks but with randomly generated measurement data, and 500 MC trials are performed on exactly the same data using the SMC-MB filter.

Fig. 10 plots the true tracks, measurements, and estimates in x and y directions versus time. The plots show that the proposed approach is able to estimate the target states. Fig. 11 shows the mean and standard deviation of the cardinality statistics versus time for both the SMC-MB filter and the proposed approach. The mean of the proposed approach also converges to the true value, and the standard deviation of the proposed approach is similar to that of the SMC-MB filter. Fig. 12 shows the average OSPA distance (when p=2 and c=200) for the SMC-MB filter and the proposed approach. The curves

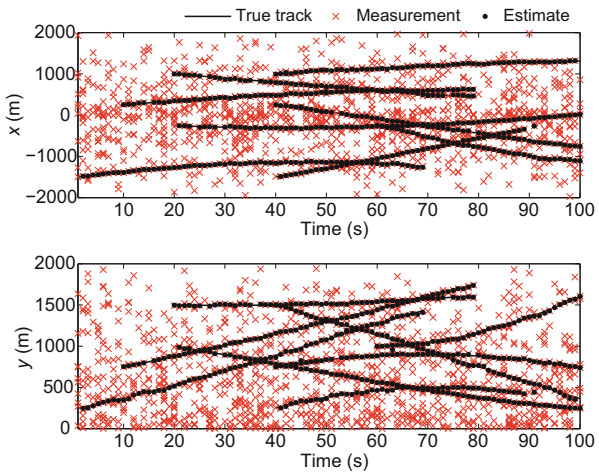

Fig. 10 True target tracks, measurements, and estimates in x and y directions versus time for the proposed approach

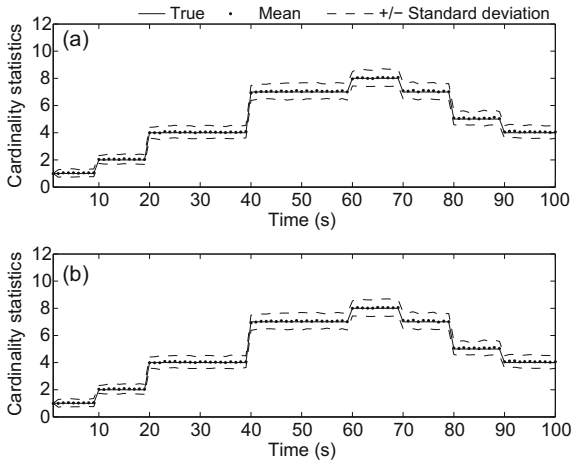

Fig. 11 The average cardinality statistics of 500 Monte Carlo runs versus time for the SMC-MB filter (a) and the proposed approach (b)

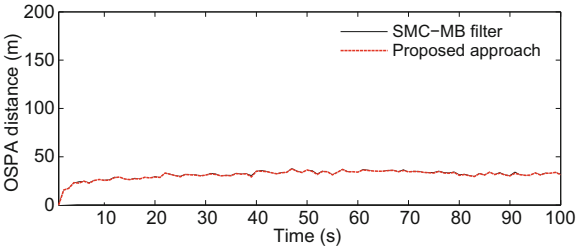

Fig. 12 The average OSPA distance for both approaches (p=2, c=200)

of the SMC-MB filter and the proposed approach almost totally overlap. This indicates that the proposed approach and the SMC-MB filter have similar filtering performance.

Table 2 gives the time averaged OSPA distance and computing time of 500 MC trials in MATLAB R2011a on a notebook with clutter density $\lambda_c = 1.6\times 10^{-3}/(\text{rad}\cdot\text{m})$. The time averaged OSPA distance of the proposed approach is almost the same as that of the SMC-MB filter. Compared with the SMC-MB filter, the proposed approach also has a larger processing rate for the nonlinear example.

Table 2 Comparison between the SMC-MB filter and the proposed approach for the nonlinear example

Filtering algorithm	Time averaged OSPA distance (m)	Average computing time (s)
SMC-MB filter	31.15	901.13
Proposed approach	31.17	404.15

5 Conclusions

In this paper, we have proposed an efficient measurement-driven approach for the SMC-MB filter. The novelty lies in the measurement-driven mechanism. The original measurements are classified using a gating technique to compute the existence probability. Since the survival and birth measurements are distinguished and most clutter measurements are eliminated, the proposed approach obtains better real-time performance. Simulations demonstrate that the proposed approach improves the real-time performance without degradation of filtering performance.

References

Bar-Shalom, Y., Li, X.R., Kirubarajan, T., 2001. Estimation with Applications to Tracking and Navigation. Wiley, New York.

Baser, E., Kirubarajan, T., Efe, M., 2013. Improved MeMBer filter with modeling of spurious targets. Int. Conf. on Information Fusion, p.813-819.

Blackman, S., Popoli, R., 1999. Design and Analysis of Modern Tracking Systems. Artech House, Norwood.

Gostar, A.K., Hoseinnezhad, R., Bab-Hadiashar, A., 2013a. Multi-Bernoulli sensor control for multi-target tracking. Proc. IEEE 8th Int. Conf. on Intelligent Sensors, Sensor Networks and Information Processing, p.312-317. [doi:10.1109/ISSNIP.2013.6529808]

Gostar, A.K., Hoseinnezhad, R., Bab-Hadiashar, A., 2013b. Robust multi-Bernoulli sensor selection for multi-target tracking in sensor networks. *IEEE Trans. Signal Process. Lett.*, **20**(12):1167-1170. [doi:10.1109/LSP.2013.2283735]

Hoang, H.G., Vo, B.T., 2014. Sensor management for multi-target tracking via multi-Bernoulli filtering. *Automatica*, **50**(4):1135-1142. [doi:10.1016/j.automatica.2014.02.007]

Hoseinnezhad, R., Vo, B.N., Vo, B.T., *et al.*, 2011. Bayesian integration of audio and visual information for multi-target tracking using a CB-MeMBer filter. IEEE Int. Conf. on Acoust Speech Signal Processing, p.2300-2303. [doi:10.1109/ICASSP.2011.5946942]

Hoseinnezhad, R., Vo, B.N., Vo, B.T., 2013. Visual tracking in background subtracted image sequences via multi-Bernoulli filtering. *IEEE Trans. Signal Process.*, **61**(2):392-397. [doi:10.1109/TSP.2012.2222389]

Li, X.R., Jilkov, V., 2003. Survey of maneuvering target tracking. *IEEE Trans. Aerosp. Electron. Syst.*, **39**(4):1333-1364. [doi:10.1109/TAES.2003.1261132]

Lian, F., Li, C., Han, C.Z., *et al.*, 2012. Convergence analysis for the SMC-MeMBer and SMC-CBMeMBer filters. *J. Appl. Math.*, Article ID 584140. [doi:10.1155/2012/584140]

Mahler, R., 2003. Multitarget Bayes filtering via first-order multitarget moments. *IEEE Trans. Aerosp. Electron. Syst.*, **39**(4):1152-1178. [doi:10.1109/TAES.2003.1261119]

Mahler, R., 2007a. PHD filters of higher order in target number. *IEEE Trans. Aerosp. Electron. Syst.*, **43**(4):1523-1543. [doi:10.1109/TAES.2007.4441756]

Mahler, R., 2007b. Statistical Multisource-Multitarget Information Fusion. Artech House, Norwood.

Ravindra, V.C., Svensson, L., Hammarstrand, L., *et al.*, 2012. A cardinality preserving multitarget multi-Bernoulli RFS tracker. Int. Conf. on Information Fusion, p.832-839.

Schuhmacher, D., Vo, B.T., Vo, B.N., 2008. A consistent metric for performance evaluation of multi-object filters. *IEEE Trans. Signal Process.*, **56**(8):3447-3457. [doi:10.1109/TSP.2008.920469]

Vo, B.N., Ma, W., 2006. The Gaussian mixture probability hypothesis density filter. *IEEE Trans. Signal Process.*, **54**(11):1091-4004. [doi:10.1109/TSP.2006.881190]

Vo, B.N., Singh, S., Doucet, A., 2005. Sequential Monte Carlo methods for multi-target filtering with random finite sets. *IEEE Trans. Aerosp. Electron. Syst.*, **41**(4):1224-1245. [doi:10.1109/TAES.2005.1561884]

Vo, B.N., Vo, B.T., Pham, N.T., *et al.*, 2010. Joint detection and estimation of multiple objects from image observations. *IEEE Trans. Signal Process.*, **58**(10):5129-5141. [doi:10.1109/TSP.2010.2050482]

Vo, B.T., 2008. Random Finite Sets in Multi-object Filtering. PhD Thesis, The University of Western Australia, Perth, Australia.

Vo, B.T., Vo, B.N., 2013. Labeled random finite sets and multi-object conjugate priors. *IEEE Trans. Signal Process.*, **61**(13):3460-3475. [doi:10.1109/TSP.2013.2259822]

Vo, B.T., Vo, B.N., Cantoni, A., 2007. Analytic implementations of the cardinalized probability hypothesis density filter. *IEEE Trans. Signal Process.*, **55**(7):3553-3567. [doi:10.1109/TSP.2007.894241]

Vo, B.T., Vo, B.N., Cantoni, A., 2009. The cardinality balanced multi-target multi-Bernoulli filter and its implementations. *IEEE Trans. Signal Process.*, **57**(2):409-423. [doi:10.1109/TSP.2008.2007924]

Vo, B.T., Vo, B.N., Hoseinnezhad, R., *et al.*, 2011. Multi-Bernoulli filtering with unknown clutter intensity and sensor field-of-view. 45th Annual Conf. on Information Sciences and Systems, p.1-6. [doi:10.1109/CISS.2011.5766180]

Vo, B.T., Vo, B.N., Hoseinnezhad, R., *et al.*, 2013. Robust multi-Bernoulli filtering. *IEEE J. Sel. Topics Signal Process.*, **7**(3):399-409. [doi:10.1109/JSTSP.2013.2252325]

Wei, J., Zhang, X., 2009. Dynamic node collaboration for mobile multi-target tracking in two-tier wireless camera sensor networks. Proc. IEEE Military Communications Conf., p.1-7. [doi:10.1109/MILCOM.2009.5379919]

Wei, J., Zhang, X., 2010a. Efficient node collaboration for mobile multi-target tracking using two-tier wireless camera sensor networks. IEEE Int. Conf. on Communications, p.1-5. [doi:10.1109/ICC.2010.5502158]

Wei, J., Zhang, X., 2010b. Sensor self-organization for mobile multi-target tracking in decentralized wireless sensor networks. IEEE Wireless Communications and Networking Conf., p.1-6. [doi:10.1109/WCNC.2010.5506184]

Williams, J.L., 2012. Hybrid Poisson and multi-Bernoulli filters. Int. Conf. on Information Fusion, p.1103-1110.

Yin, J.J., Zhang, J.Q., 2010. The nonlinear multi-target multi-Bernoulli filter using polynomial interpolation. Proc. IEEE 10th Int. Conf. on Signal Processing, p.2551-2554. [doi:10.1109/ICOSP.2010.5656888]

Yin, J.J., Zhang, J.Q., Zhao, J., 2010. The Gaussian particle multi-target multi-Bernoulli filter. IEEE 2nd Int. Conf. on Advanced Computer Control, p.556-560. [doi:10.1109/ICACC.2010.5486859]

Zheng, Y.M., Shi, Z.G., Lu, R.X., *et al.*, 2013. An efficient data-driven particle PHD filter for multitarget tracking. *IEEE Trans. Ind. Inform.*, **9**(4):2318-2326. [doi:10.1109/TII.2012.2228875]